Alpha Particle-Driven Toroidal Rotation in Burning Plasmas

M. Honda 1), T. Takizuka 1), K. Tobita 1), G. Matsunaga 1), A. Fukuyama 2), T. Ozeki 1)

1) Japan Atomic Energy Agency, Naka, Ibaraki, Japan
2) Graduate School of Engineering, Kyoto University, Sakyo-ku, Kyoto, Japan

e-mail contact of main author: honda.mitsuru@jaea.go.jp

Abstract. The mechanism of a torque intrinsically produced by alpha particles and the subsequent possibility to create significant toroidal rotation and shear are investigated. In DEMO plasmas, an orbit-following Monte Carlo code OFMC predicts that the profile of a collisional torque is influenced near the magnetic axis by a reversed magnetic shear configuration, while that of a $\vec{j} \times \vec{B}$ torque is not. It is found that the gradient of the source profile of alpha particles produces the co-directed collisional torque and a counter-directed $\vec{j} \times \vec{B}$ torque, and both torques virtually cancel each other out in the central region of the plasma. A non-negligible torque shear and resulting toroidal rotation in the co-direction are obtained in a weakly reversed-shear configuration, but the estimated rotation velocity is below the threshold to stabilize resistive-wall modes through intrinsic alpha-driven torque alone.

1. Introduction

Toroidal rotation and shear play an important role in suppressing turbulent transport and MHD instabilities not only in plasmas observed in current tokamak experiments but also in burning plasmas estimated for ITER and DEMO. In current devices toroidal rotation can be driven and controlled with a tangentially-injected neutral beam (NB) through a collisional slowing-down momentum transfer process involving passing particles. However, it is now commonly believed that we will have limited means to drive and control toroidal rotation especially in DEMO because self-generated alpha particle heating will be dominant. Therefore, few external heating systems may be expected to be installed; port openings for these systems in a vacuum vessel take up space that potentially reduces the tritium breeding ratio (TBR) below unity, indicating that a self-sufficient, fuel-generating plasma is no longer feasible. In addition, collisional momentum transfer from tangential NBIs would not be significant in the core region of a DEMO plasma: first, the beam energy E_b is higher than that used in current devices, such that the momentum input expressed by $\sim P_\mathrm{b}/E_\mathrm{b}^{1/2}$ becomes smaller, where P_b denotes the beam power. In SlimCS [1], one of the DEMO concepts, only NBI and ECH systems are planned to be installed and $E_\mathrm{b} \lesssim 1.5\,\mathrm{MeV}$ is expected, which is around 18 times higher than that of positive NBIs in JT-60U. Secondly, the high density of the plasma results in a short mean free path of beam ions. These beam ions are likely to be trapped in the outboard region of the plasma, leading to a decrease in the number of passing particles in the core region. In this sense, in order to evaluate the impact of toroidal rotation on turbulence and MHD instability, we first should explore the potential of an intrinsic torque source in self-sustained burning plasmas.

In this paper we focus on torque and toroidal rotation solely stemming from alpha particles despite several other possible intrinsic torque sources in burning plasmas. To our knowledge, only a few papers discuss alpha-driven toroidal rotation and/or torque [2, 3, 4, 5]. Rosenbluth and Hinton, analytically solving equations of motion and Fokker-Planck equations for extreme cases, conclude that rotation and its shear sufficient to suppress instabilities may be impossible in a tokamak reactor [3] because, in general, the frictional and the $\vec{j} \times \vec{B}$ torques cancel out if the alpha orbits are well-confined. Schneider et al. illustrate that the $\vec{j} \times \vec{B}$ torque will be invoked by alpha particles [4], but the main body of their work focuses primarily on an alpha-driven current, not rotation, similar to the work of Tani and Azumi [6]. Test-particle simulations with a Solove'v equilibrium by Thyagaraja et al. clearly show that a positive fast-ion radial current does flow in ITER, pushing a bulk plasma in a direction counter to the plasma current [5]. As

a result, they state that counter-current NBIs should be installed in ITER to enhance counter-toroidal rotation. However, their work ignores the contribution of collisional alpha-particle torque, which may offset collisionless (radial current) torque, as Rosenbluth and Hinton state [3].

Based on the preceding research, we now investigate an intrinsic torque stemming from the motion of alpha particles born from fusion reactions and the resulting toroidal rotation in SlimCS plasmas, using an orbit-following Monte Carlo code OFMC [7]. A DEMO plasma with internal transport barriers (ITBs) in a weakly reversed shear (W-RS) configuration is generally anticipated to exist in a steady state because these conditions are necessary to sustain a high bootstrap current fraction. Density and temperature profiles determine the birth profile of alpha particles, and alpha orbits conform to the magnetic configuration, both of which have a significant impact on the torque profile. In this sense, we have to consider realistic conditions regarding the magnetic configuration and the source profile of alpha particles of a DEMO plasma, a focus which clearly distinguishes our study from preceding work.

2. Alpha Particle Orbit

In burning plasmas with deuterium and tritium equally mixed, alpha particles are constantly born due to D-T fusion reactions. This process actually creates no accompanied electrons unlike the ionization of fast neutrals by NBIs: collisions between ionized deuterium and tritium produce a charged alpha particle, i.e., a fast helium ion, and a neutron. In terms of quasi-neutrality, however, we may regard the two electrons adjacent to the fusion reaction as accompanied electrons of the fusion reaction, because they practically offset the charges of the deuterium and tritium ions. These electrons remain at the surface where the reaction occurs, while a fusion-born alpha particle deviates from the surface due to drift motion. The maximum deviation of a collisionless alpha particle is about $\sim \epsilon^{1/2}\rho_p$ for trapped particles and $\sim \epsilon\rho_p$ for passing ones, where ϵ is the inverse aspect ratio and ρ_p the poloidal Larmor radius. Because ρ_p is proportional to $T_{\rm i}^{1/2}$ and inversely proportional to B_θ, where $T_{\rm i}$ is the ion temperature and B_θ the poloidal magnetic field, we expect that a trapped alpha particle with 3.5 MeV in the core region of a reversed shear (RS) plasma has a deviation width much wider than those of any other category. This charge separation between alpha particles and electrons must generate a fast-ion radial current. Owing to the large dielectric constant of a fusion plasma, an opposite radial current driving toroidal rotation emerges in the plasma. Unlike directional NBIs, however, alpha particles are isotropically born at the moment of their birth in general. This fact indicates that it is not straightforward to determine the direction of the $\vec{j}\times\vec{B}$ torque or whether the torque integrated over the entire volume is finite or not. A similar case holds for collisional torque. Isotropic birth means that particles are born with an equal probability of having any pitch angles. The likely result may seem at first to be no net collisional torque as a whole.

When considering finite orbit widths and the parabolic source profile of alpha particles, however, we anticipate finite collisional and $\vec{j}\times\vec{B}$ torques; in other words, alpha particles have directional characteristics. The preceding analytical studies clarify that the trapping boundary is asymmetric in a parallel velocity $V_\parallel$ near the magnetic axis [8], indicating that the trapping ratio for particles with a negative $V_\parallel$ is higher than that for particles with a positive $V_\parallel$, and the trapping boundary no longer exists for co-moving particles with sufficiently high energies [9]. These studies indicate that co-passing alpha particles are predominant, at least near the magnetic axis, due to the finite-orbit-width effect. Numerical analyses of alpha particles in JET also show an excess of co-passing particles relative to counter-passing ones [10]. The source of alpha particles is proportional to the square of both density and temperature of a bulk plasma, so that the profile is centrally peaked and localized in the core region. In other words, particles born on a surface outnumber those born on any outward adjacent surface in the core region.

This gradient of the source profile leads to a co-directed particle flow and an outward fast-ion radial current due to the finite-orbit-width effect. These issues concerning the orbit of alpha particles will be considered in detail in the following sections using numerical simulations.

3. Physics of Alpha Particle-Induced Torque

OFMC was recently updated to enable estimation of the $\vec{j} \times \vec{B}$ torque, as well as collisional torque. OFMC is thus employed to study the alpha particle-induced torque profile formed in a normal shear (NS), a weakly reversed shear (W-RS) and a reversed (negative) shear (RS) configuration. These equilibria are designed for SlimCS plasmas and are obtained by solving the Grad-Shafranov equation numerically using an equilibrium code MEUDAS [11]. The chief parameters of SlimCS plasmas are as follows: the major radius $R = 5.63\,\mathrm{m}$, the minor radius $a = 2.1\,\mathrm{m}$, the toroidal magnetic field $B_\phi = 6.0\,\mathrm{T}$, the plasma current $I_\mathrm{p} = 16.7\,\mathrm{MA}$, the ellipticity $\kappa = 2.1$ and the triangularity $\delta = 0.4$. In general, it is hard numerically to find the equilibrium of a DEMO plasma with both a strong RS and ITBs at the same time. Only in this section, as inputs for OFMC, do we use density and temperature profiles with ITBs that are not identical to the pressure profile used in the equilibrium solver; rather, this approach is advantageous because we easily can understand the physical origin of the observed results by varying a pressure profile or magnetic shear individually. We then focus on the physics of the impact of the magnetic configuration on the behavior of alpha particles.

The safety factor q profiles corresponding to the NS, W-RS and RS configurations are shown in Fig. 1. A strong RS configuration may not be realistic for a DEMO plasma. Nevertheless, it is useful to study the behavior of alpha particles running through a low B_θ region. OFMC follows $400,000$ test particles until they slow down. Details of how to numerically deal with alpha particles in OFMC have been found in Ref. [6]. Figure 2 displays the profiles of the collisional and $\vec{j} \times \vec{B}$ torques and their total as well as the source profile of alpha particles S_α that depends on the background density and temperature profiles. Characteristics in common among the three cases include: (1) a co-directed collisional torque and a counter-directed $\vec{j} \times \vec{B}$ torque appear over the entire region, (2) both torques cancel each other out beyond $r/a \approx 0.5$, i.e., no net torque, while (3) co-torque appears near the magnetic axis due to the influence of the co-collisional torque, and (4) the location of the maximum magnitude of both torques is nearly identical to that of the maximum gradient of S_α. In contrast, a clear difference among the three cases is found in that the amount of collisional torque in the co-direction near the axis increases as q is increasing, while the $\vec{j} \times \vec{B}$ torque in the corresponding region seems to be hardly affected by q. We will carefully consider these points in the following.

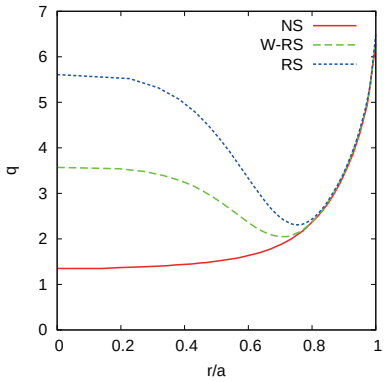

FIG. 1. The q profiles in the NS, W-RS and RS configurations calculated by MEUDAS.

The preceding studies and our simulations regarding particle orbits, both confirm an excess of co-directed particles due to co-collisional torque over the entire region. From Fig. 2, it seems that the reason for the predominance of co-collisional torque differs from area to area. Focusing first on the region near the magnetic axis, we observe no significant gradient of the source profile compared to that for the other region, and clearly the magnitude of the co-collisional torque becomes larger as q increases, conceivably due to the magnetic topology rather than the source profile. To confirm this speculation, we carry out orbit-following simulations during a one bounce period. Because we assume for this time only a collisionless plasma with no ripple field, all the test particles must return to where they are born, with their orbits closed in

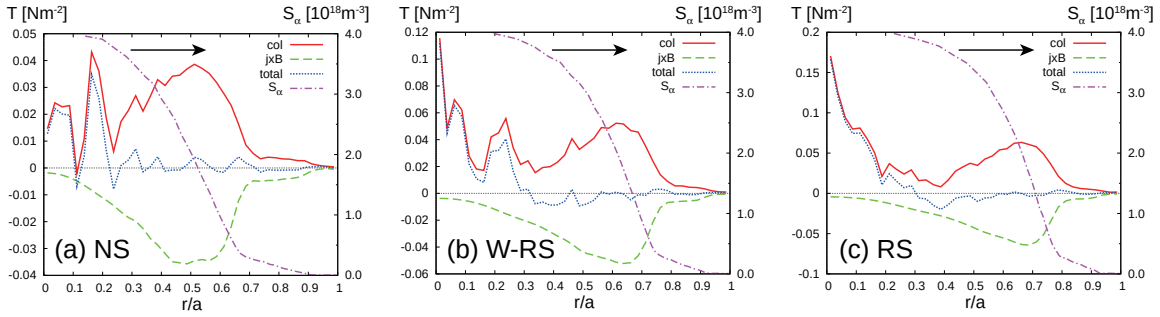

FIG. 2. Profiles of the collisional (col) and $\vec{j} \times \vec{B}$ (jxB) torques and their total (total) in the (a) NS, (b) W-RS, and (c) RS configurations. The source profiles of alpha particles (S_α) are also shown for each case.

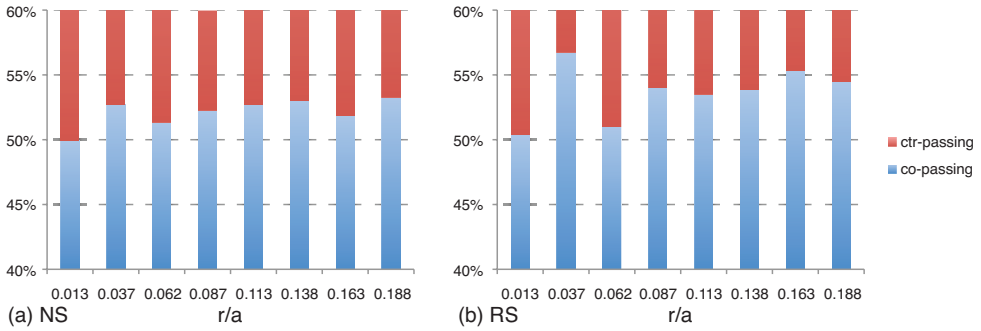

FIG. 3. The ratio of counter- and co-passing test particles relative to all passing particles near the magnetic axis in the (a) NS and (b) RS configurations.

a bounce. In doing so, after following the orbits of all test particles during a bounce period, we are able to count exactly the number of test particles categorized as co or counter and as passing or trapped. We note that even though a collisionless plasma is just an assumption, a burning plasma is almost collisionless due to its very high temperature. Figure 3 shows the radial profiles of the ratio of counter- and co-passing test particles to their total for the (a) NS and (b) RS configurations. In both cases co-passing particles actually outnumber counter-passing ones, but in case (b) the ratio of co-passing particles is larger than that in case (a) for almost every region near the axis. This fact implies that collisional slowing-down and pitch-angle scattering processes do not create asymmetry in the co- and counter-directions, but that magnetic topology does. This finding also can be readily confirmed by drawing collisionless orbits with various pitch angles in the RS configuration, as shown in Fig. 4. When focusing on orbits of particles born on the $\psi = 0.01$ surface on the low-field-side (LFS), we find that particles with co-directed pitch angles at birth are confined inside $\psi \approx 0.01$, as shown in Fig. 4 (a), while some of those with counter-directed pitch angles drift across the $\psi = 0.1$ surface, as shown in Fig. 4 (b), because they are no longer passing particles. As a whole, co-collisional torque dominates inside $\psi = 0.1$ for particles born on the LFS. In contrast, particles with co-directed pitch angles born on the HFS tend to go outward from the surface of their birth, and those with counter-directed pitch angles tend to go inward, as shown in Figs. 4 (c) and (d). However, some of the counter particles become trapped. This finding is expected, given the greater number of co-passing particles relative to that of counter-passing ones inside $\psi = 0.1$, even on the HFS. This is also the case for the NS configuration, but to a lesser extent: co-passing particles outnumber counter-passing ones and co particles are rarely trapped, compared to counter ones. Schneider et al. in a straightforward manner explain the reason for the excess of co-passing particles in the RS configuration using the concept of the conservation of toroidal angular momentum [4].

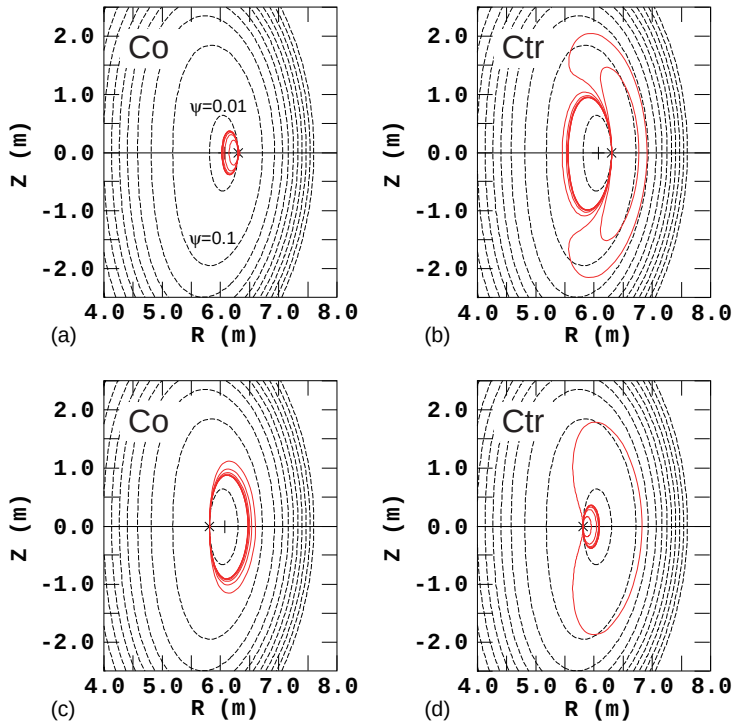

FIG. 4. Collisionless orbits of (a) co- and (b) counter-particles born at the midplane of the $\psi = 0.01$ surface on the LFS of the RS plasma. Cases (c) and (d) are equivalent to cases (a) and (b) except for the HFS, respectively. In each figure eight orbits are drawn with pitch angles from 10° to 80° at 10° intervals for cases (a) and (c) and from 100° to 170° for cases (b) and (d).

In Fig. 2, the source profiles S_α are all parabolic, i.e., they have more or less a finite gradient over the entire profiles. In order to distinguish the effects of a finite gradient of S_α from those caused by other factors, we artificially assume that the profile of S_α is flat in the core region and steep in the edge region, i.e., a box-type profile. We carry out simulations with the same conditions as in Fig. 2 except for S_α. We expect that both the collisional and $\vec{j}\times\vec{B}$ torques will be prominent near the region where S_α is steep and be small in the other region, provided that the gradient of S_α causes both torques in Fig. 2 to increase in magnitude. Figure 5 clearly shows that for all cases, collisional torque is negligible in the central region where $0.3 \lesssim r/a \lesssim 0.6$, and regions with a steep S_α gradient coincide with those of prominent collisional and $\vec{j}\times\vec{B}$ torques. In addition, the shape and magnitude of the collisional torque inside $r/a \approx 0.2$ are nearly equivalent to those in Fig. 2, which also supports the fact that co-passing particles near the axis are predominant due to the magnetic topology, not S_α. Moreover, the relative absence of any collisional torque in the central region indicates that collisional torque is offset by isotropy of alpha particle generation, with the exception of proximity to the axis and the finite gradient of S_α.

In order to identify why the gradient of S_α produces a co-collisional torque and a counter-$\vec{j}\times\vec{B}$ torque, we should focus on the trapped orbits in the corresponding regions. Figure 6 shows co- and counter-trapped orbits born at $\psi = 0.4$ and those at $\psi = 0.5$. We imagine a situation in which there is a steep gradient of S_α between these ψ surfaces. For example, let us assume that 100 test particles are generated at the point denoted by a cross in Fig. 6, and 10 test particles at the point denoted by an open square, based on speculation using the S_α profile in the figure. In the case in which co-trapped and counter-trapped particles are equally generated at both points, counter-trapped particles born at the cross symbol move outward in the region between the $\psi = 0.4$ and 0.5 surfaces, while co-trapped particles born at the open square symbol move inward in the same region. These contributions cancel each

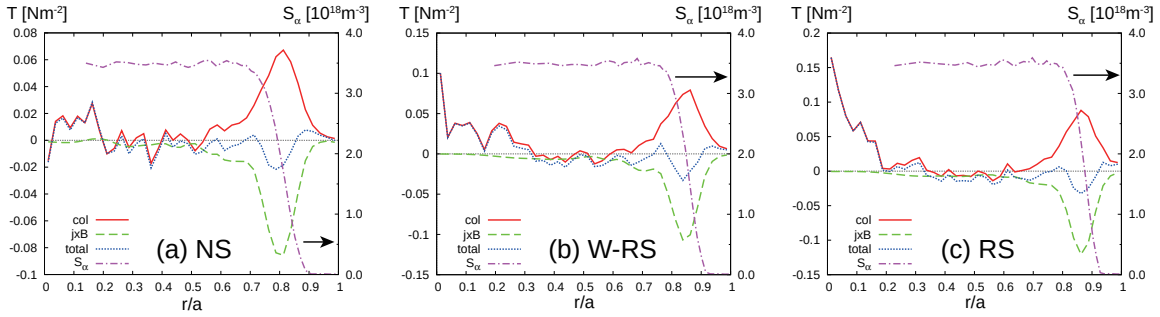

FIG. 5. Profiles of the collisional (col) and $\vec{j}\times\vec{B}$ (jxB) torques and their total (total) in the (a) NS, (b) W-RS, and (c) RS configurations with the S_α profiles artificially held flat in the core and precipitous in the edge regions.

other, and a net 45 test particles moves outward, producing an outward fast-ion radial current. An inward ion radial current flowing in the opposite direction subsequently creates a $\vec{j}\times\vec{B}$ torque that drives counter rotation in the plasma. During the outer leg of the bounce motion of counter-trapped particles, they actually move in a co-direction toroidally. Focusing on the $\psi = 0.5$ surface, we find that the counter-particles born at the cross symbol deposit their co-collisional torque on the surface, which tends to be offset by the deposited counter-collisional torque of the particles born at the open square symbol, and that the particles born at the outward adjacent surface, e.g., $\psi = 0.6$, give their counter-torque to the surface. The source gradient enhances the contribution from the inboard trapped particles, resulting in a co-directed collisional torque. In practice, the fact that there are to a certain extent more counter-trapped particles generated than co-trapped ones, as already noted, reinforces co-collisional torque and a counter $\vec{j}\times\vec{B}$ torque. We deduce that a $\vec{j}\times\vec{B}$ torque exceeds collisional torque in the steep S_α region due to the role of trapped particles: a $\vec{j}\times\vec{B}$ torque is produced mainly by trapped particles, while collisional torque is not.

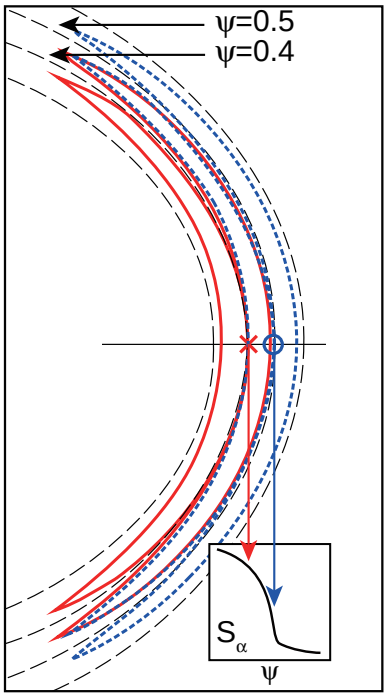

FIG. 6. Trapped orbits born at $\psi = 0.4$ (solid lines) and those born at $\psi = 0.5$ (dotted lines). The lower right figure shows a schematic drawing of the steep S_α profile. The horizontal scale of the figure is stretched doubly.

4. Alpha Particle-Induced Torque in SlimCS plasmas

In this section, we estimate the torque induced by alpha particles and the resulting toroidal rotation in SlimCS plasmas. Equilibria in the NS and W-RS configurations are constructed using the ACCOME code [12] that is able to solve the Grad-Shafranov equation consistent with arbitrarily given density and temperature profiles and a current density profile driven by several current-drive methods. The given pressure profiles and the resultant q profiles are exhibited in Fig. 7 (c), and the simulation results regarding the torque are shown in Figs. 7 (a) and (b). The overall tendencies are similar to those in Fig. 2. The net torque input of alpha particles is summarized in Table I, showing that for both cases no net torque virtually emerges because both torques almost exactly cancel each other out. Even though the contribution of each to total torque is significant, alpha-driven torque does not become significant due to cancellation. We note that this finding supports the conservation law of toroidal angular momentum. For the W-RS case, however, a clear torque shear is found in the

TABLE I. Collisional and $\vec{j}\times\vec{B}$ torques and their total integrated over the entire volume, in [Nm] units.

	coll. torque	$\vec{j}\times\vec{B}$ torque	total
(a) NS	10.87	−10.87	$-2.33\,10^{-3}$
(b) W-RS	12.13	−12.34	$-2.07\,10^{-1}$

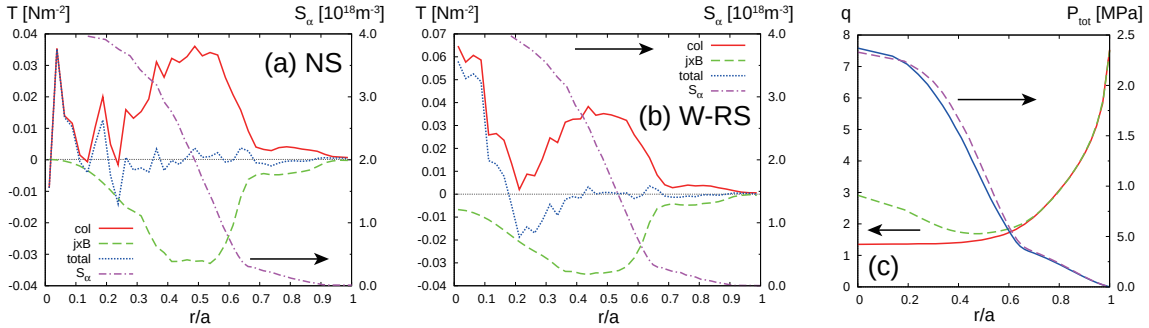

FIG. 7. Profiles of the collisional (col) and $\vec{j}\times\vec{B}$ (jxB) torques and their total (total) in the (a) NS and (b) W-RS configurations with the S_α profiles in SlimCS. The corresponding q and the pressure profiles $P_{\rm tot}$ are shown in (c), denoted by solid lines for case (a) and broken lines for case (b).

core region owing to the effect of the magnetic field, despite no net torque. This sheared torque is expected to produce sheared toroidal rotation and to remain constantly so.

The multi-fluid transport code TASK/TX is a 1D transport code to calculate self-consistently the evolution of a plasma, including the radial electric field and the rotations [13]. Utilizing this code together with the torque profiles calculated by OFMC, for both cases we now roughly estimate a toroidal rotation profile driven solely by the alpha particle-induced torque. We assume that momentum diffusivity is equivalent to the thermal diffusivity calculated by the CDBM model [14] and neglect momentum convection, for the sake of simplicity. Time-dependent simulations at a steady state are carried out to obtain the toroidal rotation of a burning plasma with the density, temperature and current density profiles used by ACCOME.

Toroidal rotation profiles at a nearly steady state in SlimCS are shown in Fig. 8 for the NS and W-RS cases: the rotation profiles almost reach a steady state at $t = 1$ s with the temperature profiles fixed and the density profile nearly unchanged. In the W-RS configuration, the plasma attains a modestly rapid co-toroidal rotation near the axis owing to both the torque profile, shown in Fig. 7 (b), and the suppression of turbulence. A decrease in momentum diffusivity in the core region makes the rotation profile very similar to the torque profile. In contrast, significant rotation near the axis is not seen for the NS case. Experimental breakthroughs regarding resistive-wall modes (RWMs) demonstrate that an observed threshold of toroidal rotation sufficient to stabilize RWMs is around 0.3% of the Alfvén velocity v_A [15]. In our cases $v_A \approx 6.33\times10^3$ km/s in the core region, 0.3% of which is equal to 19.0 km/s. Focusing on the velocity at the surface where $q = 2$, we find at most −1.0 km/s in Fig. 8, which is far below the threshold.

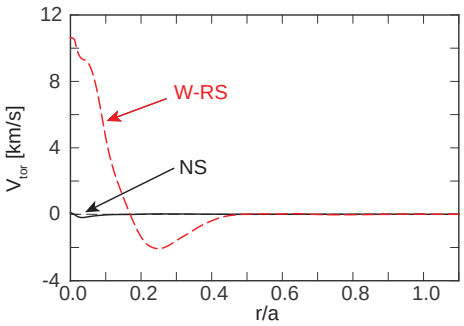

FIG. 8. Toroidal rotation profiles for the NS and W-RS cases at $t = 1$ s after initiation.

5. Conclusions

We have numerically investigated toroidal rotation driven by the torque due solely to alpha particles in SlimCS plasmas, using the OFMC code. Although alpha particles are born isotropically, they have intrinsic asymmetry in the co- and counter-directions due to finite orbit widths, near the core region. Simulations by OFMC reveal this tendency in three magnetic configurations and disclose some physical characteristics. Co-collisional torque becomes more prominent as the magnetic shear becomes more negative in the corresponding region. This fact can be confirmed by counting co- and counter-passing particles and drawing their orbits based on the proximity of their birth to the magnetic axis, the latter of which clearly shows the anisotropy of alpha particles under the influence of a magnetic field. In contrast, the $\vec{j}\times\vec{B}$ torque, which is always negative over the entire profile, is insensitive to the magnetic configuration. The gradient of the source profile of alpha particles is found to be a strong driver in generating co-collisional torque and a counter $\vec{j}\times\vec{B}$ torque. Collisional torque and the $\vec{j}\times\vec{B}$ torque effectively cancel each other out in regions where both contributions are negligible.

More realistic SlimCS plasmas in which density, temperature and current density profiles are consistent with equilibria are calculated by the ACCOME code to estimate torque and the toroidal rotation profile. The net torque due to alpha particles is negligible, because co-collisional torque is in large measure offset by a counter $\vec{j}\times\vec{B}$ torque. With the transport code TASK/TX, a profile of toroidal rotation induced by alpha particles is predicted for both the NS and W-RS cases, using the torque profile from OFMC as an input. Estimated toroidal rotation does not meet the threshold velocity for stabilizing RWMs. Rotation above the threshold would be attainable if the NBI were to assist at a much higher energy level compared to current NBIs.

This work was supported by a Grant-in-Aid for Young Scientists (B) (No 22760667) from the Japan Society for the Promotion of Science (JSPS).

References

[1] TOBITA, K., et al., Nucl. Fusion **47** (2007) 892.

[2] KOLESNICHENKO, Y.I., YAKOVENKOR, Y.V., Fusion Technology **18** (1990) 597.

[3] ROSENBLUTH, M.N., HINTON, H.L., Nucl. Fusion **36** (1996) 55.

[4] SCHNEIDER, M., et al., Plasma Phys. Control. Fusion **47** (2005) 2087.

[5] THYAGARAJA, A., SCHWANDER, F., McCLEMENTS, K.G., Phys. Plasmas **14** (2007) 112504.

[6] TANI, K., AZUMI, M., Nucl. Fusion **48** (2008) 085001.

[7] TANI, K., et al., J. Phys. Soc. Jpn. **50** (1981) 1726.

[8] CHU, T.K., Phys. Plasmas **3** (1996) 3397.

[9] CHIU, S.C., CHAN, V.S., OMELCHENKO, Y.A., Phys. Plasmas **9** (2002) 877.

[10] EGEDAL, J., Nucl. Fusion **40** (2000) 1597.

[11] AZUMI, M., et al., Proc. 4th Int. Symp. on Comput. Methods Applied Sci. Engineering, Paris (North-Holland, Amsterdam, 1980) 335.

[12] TANI, K., AZUMI, M., DEVOTO, R.S., J. Comput. Phys. **98** (1992) 332.

[13] HONDA, M., FUKUYAMA, A., J. Comp. Phys. **227** (2008) 2808.

[14] FUKUYAMA, A., et al., Plasma Phys. Control. Fusion **37** (1995) 611.

[15] TAKECHI, M., et al., Phys. Rev. Lett. **98** (2007) 055002.